

Article

Preparation of a New Shape-Stable Phase-Change Material Based on Expanded Perlite, Paraffin, Epoxy, Copper and High-Density Polyethylene

Linda Gouissem ^{1,2,*} and Farid Rouabah ^{3,4}

¹ Département d'Enseignement de Base en Technologie, Faculté de Technologie, Université Ferhat ABBAS Sétif-1, Setif 19000, Algeria

² Laboratoire Préparation, Modification et Application des Matériaux Polymériques Multiphasiques (LPMAMPM), Institut des Sciences et Techniques des Matériaux, Université Ferhat ABBAS Sétif 1, Setif 19000, Algeria

³ Institut des Sciences et Techniques des Matériaux, Université Ferhat ABBAS Sétif 1, Setif 19000, Algeria; f_rouabah2002@univ-setif.dz (F.R.)

⁴ Laboratoire Physico-Chimie des Hautes Polymères (LPCHP), Institut des Sciences et Techniques des Matériaux, Université Ferhat ABBAS Sétif 1, Setif 19000, Algeria

* Corresponding author. E-mail: 1566gl@gmail.com or linda.gouissem@univ-setif.dz (L.G)

Received: 22 September 2024; Accepted: 13 December 2024; Available online: 20 December 2024

ABSTRACT: Phase change materials (PCMs) face challenges such as low thermal conductivity and leakage, often addressed through attempts at encapsulation or integration into polymer matrices or porous materials. This study uses expanded perlite to prepare a PCM composite. The perlite is treated with hydrochloric acid to remove impurities and improve its absorption, then impregnated with paraffin at 65 °C, with the addition of copper to enhance thermal conductivity. After drying, the material was coated with epoxy resin to prevent leakage and mixed with high-density polyethylene (HDPE) to improve its mechanical strength and facilitate integration with other materials. Characterization techniques, including differential scanning calorimetry (DSC), thermogravimetric analysis (TGA), and scanning electron microscopy (SEM), evaluate the structure and properties of the composite. TGA results show that acid treatment increases paraffin absorption to 80% by weight, while weight loss tests confirm the effectiveness of the epoxy coating against leaks. A decrease in melting temperatures was observed in all HDPE blends, ranging from 4.72 °C to 9.58 °C, likely due to the integrated elements interfering with the reorganization of the molecular chains of HDPE. Although the preparation improved thermal conductivity, thermal tests revealed that increasing the (perlite/PCM) phase in HDPE is essential for further optimization, highlighting the potential of the composite as an effective energy storage solution for sustainable systems.

Keywords: Composite; Energy storage; Expanded perlite; Thermal conductivity; Paraffin; High-density polyethylene; Phase change material



© 2024 The authors. This is an open access article under the Creative Commons Attribution 4.0 International License (<https://creativecommons.org/licenses/by/4.0/>).

1. Introduction

Technological and economic advancements driving societal progress worldwide are leading to an increase in energy demand. Global energy consumption, as well as CO₂ and greenhouse gas emissions, are experiencing a dramatic acceleration due to the growth of the global population, the pace of economic growth, and the increasing reliance on high-energy-consuming devices [1]. The majority of energy consumption is derived from fossil fuels, which are finite and cause significant environmental pollution and climate change. Consequently, the efficient utilization of energy has become a major concern, resulting in a trend towards the use of sustainable and renewable energy resources. These resources are abundant, accessible, and environmentally friendly. Thermal energy storage (TES) is a promising solution that is rapidly developing [2]. The construction sector has a major influence on total energy consumption worldwide, and this increase is due not only to the production of building materials and the construction of buildings, but above all to the operation of buildings [3]. According to research, approximately 30% of total energy consumption can be

attributed to the energy used in building operations aimed at maintaining indoor comfort [4]. This situation has created a growing need for the development of new, clean, and sustainable energy conversion and storage systems. TES is a promising and sustainable method to reduce energy consumption in the building sector. TES systems using phase-change materials (PCMs) have many applications for providing and maintaining a comfortable environment in the building envelope without the consumption of electrical energy or fuel [5].

Phase-change materials (PCMs) are substances capable of absorbing and storing large quantities of thermal energy. The mechanism of PCMs for energy storage is based on the increased energy requirement of certain materials to undergo a phase transition. They are able to absorb sensible heat as their temperature increases and, at the phase-change temperature, absorb a large amount of heat, known as the latent heat of fusion, in order to change phase. The energy remains stored in the PCM until the temperature drops and the material undergoes another phase transition, which also means the release of energy [1]. PCMs are widely used in construction to enhance energy efficiency. Integrated into walls, ceilings, and roofs, they regulate indoor temperatures by storing and releasing thermal energy, reducing the need for heating and cooling systems [6–9]. Beyond building applications, PCMs are also utilized in cooling systems, heat transfer technologies, and thermal protection devices [10,11]. Additionally, they are incorporated into foam materials to improve insulation properties [12,13] and thermoplastics like asphalt to regulate surface temperatures, enhancing durability [14–16]. PCMs are primarily solid-liquid materials and can be categorized as organic (e.g., paraffin and fatty acids) or inorganic (e.g., hydrated salts and metals) [17]. Organic PCMs are preferred for building applications due to their stability and safety, but they face challenges like low thermal conductivity and potential liquid-phase leakage.

To address these issues, researchers have developed composite PCMs. One widely studied approach is encapsulating PCMs with thermally conductive materials, which prevents leakage, protects against corrosion, and enhances heat transfer. Another method involves creating form-stable composites, where PCMs are embedded within cross-linked polymer matrices, porous mineral materials, or expanded graphite or perlite [3,5,18].

Several studies have been conducted to develop new composite materials for thermal energy storage based on PCMs. For instance, the work of S. Ramakrishnan et al. [19], involved the development of a new thermal energy storage composite based on expanded perlite filled with RT21 paraffin and coated with silicone. This composite, containing up to 50% paraffin, exhibited complete impermeability when inserted in concrete and showed a significant improvement in thermal inertia and thermal energy storage. N. Mekaddem et al. [20] also studied expanded perlite filled with RT27 paraffin and coated with a waterproof polymer (Sikalatex), mixed with plaster and 10% by weight of aluminum powder to enhance the thermal conductivity of the composite. They found that the paraffin loading rate was 60% by weight, and the composites with and without aluminum had acceptable thermal storage capacities, making them suitable for regulating indoor building temperatures. As for L. Bayés Garcia et al. [21], they focused on paraffin as a phase change material. They prepared microcapsules of paraffin coated with films made from a mixture of gelatin/arabic gum and agar-agar/arabic gum. They found that the microencapsulated PCMs prepared were fully capable of fulfilling their role in thermal energy storage.

This study focuses on the preparation of a stable phase-change composite material incorporating expanded perlite (ExP), paraffin (PCM), copper (Cu), epoxy resin (Ep), and high-density polyethylene (HDPE). The adopted methodology consists of two main steps. The first step encompasses several sub-steps, namely the melting of the paraffin, with or without the addition of copper powder, followed by its insertion into the pores of the ExP through direct impregnation. The resulting mixture is then coated with an epoxy resin. The second step involves mixing the prepared composites, namely: (PCM/ExP), (PCM/ExP/Ep), and (PCM/ExP/Cu/Ep), with the HDPE at various volume percentages. This work presents an innovative contribution to energy storage research, as the use of expanded perlite as a container for paraffin and epoxy resin to prevent leakage has not been sufficiently explored in the existing scientific literature. Furthermore, the integration of HDPE acts not only as a secondary container but is also expected to improve the mechanical properties of the composite.

2. Materials and Methods

2.1. Materials

The phase-change material (PCM) used in this study is RT55 paraffin, supplied by Rubotherm, having the characteristics summarized in Table 1 [22]. The expanded perlite used was supplied by TAOUAB Construct (Kouba, Algeria), and its main chemical constituents were determined using an X-ray fluorescence spectrometer (XRF, JSX-3201Z, JEOL, Tokyo, Japan) and are presented in Table 2, while its characteristics are summarized in Table 3 [23]. In contrast, the epoxy used (HS AUTO EPOXY) is a two-component epoxy compound for industrial floor protection,

supplied by Purepox (Tipaza, Algeria). As for HDPE F00952, supplied by Sabic (Riyadh, Saudi Arabia), it has a melt index of 0.07 g/10 min (190 °C, 2.16 kg), according to ISO 1133, and a density of 0.95 g/cm³ [24].

Table 1. RT55 properties according to Rubitherm GmbH [22].

Properties	Values
Melting zone	51–57 (°C)
Solidification zone	56–57 (°C)
Heat storage capacity ±7.5%	170 (kJ/kg)
Specific heat capacity	2 (kJ/kg·K)
Solid density at 15 °C	0.88 (kg/L)
Liquid density at 80 °C	0.77 (kg/L)
Thermal conductivity (both phases)	0.20 W/(m·K)
Volume expansion	14 (%)
Flash point	>200 (°C)

Table 2. Chemical composition of expanded perlite.

Constituent	SiO ₂	Al ₂ O ₃	Fe ₂ O ₃	CaO	Na ₂ O	K ₂ O	MgO
Rate (%)	71.4	10.0	2.08	2.94	3.85	9.25	0.163

Table 3. Expanded perlite characteristics according to TAOUAB data sheet [23].

Property	Value
Apparent density	50–80 kg/m ³
Compacted density	60–100 kg/m ³
PH value	7–9
color	White
Quantity of SiO ₂	60–80%

2.2. Methods

Figure 1 presents the experimental protocol used in this study, highlighting the successive steps involved in the preparation of the composites. These steps include the treatment of raw materials, such as expanded perlite with hydrochloric acid and paraffin, followed by their incorporation into the polymer matrix. The protocol also covers the characterization techniques applied to the constituent materials and the final composites, aiming to deepen the understanding of their properties and behavior. The details of each step will be described in the following sections.

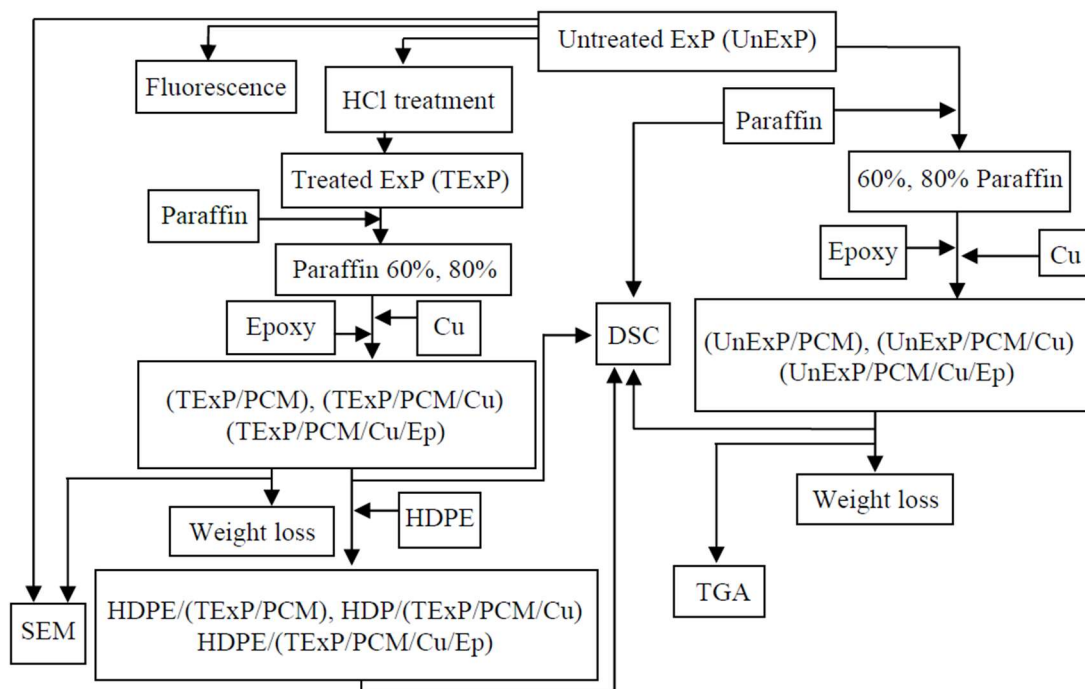


Figure 1. Protocol for the preparation and characterization of composites and their constituent materials.

The microporous structure of perlite requires chemical pre-treatment with hydrochloric acid to increase its internal surface area, porosity and surface activity.

The acid treatment process is performed as follows:

After drying at 100 °C for 2 h, the perlite is immersed in a 10% hydrochloric acid solution for 12 h. Next, NaOH 0.1 N is added to neutralize the perlite down to pH 7, after which the perlite is washed several times with distilled water, filtered and then calcined at 500 °C for 2 h. In this way, impurities and residual moisture are removed from the perlite surface, and the pore structure is activated. The impregnation capacity of treated (TExP) and untreated perlite (UnExP) has been evaluated and verified.

2.2.1. Step 1: Impregnation of Perlite by Paraffin

1. Perlite is dried at 100 °C for 24 h.
2. 60 g of RT55 paraffin are placed in a beaker and then in a water bath at 65 °C. After melting, 40 g of expanded perlite are added progressively and mixed carefully with a spatula for 5 min. After that, the beaker is removed from the water bath and mixing continues with a propeller blender for a further 5 min to obtain a mixture noted F1 (*i.e.*, 60% by weight of paraffin) (see Figure 2).
3. A second mixture is prepared with 80 g RT55 and 20 g perlite under the same conditions. (*i.e.*, 80% by weight), noted F2.
4. A third mixture is prepared based on F1 or F2 with 0.4% by volume of Cu powder, these mixtures are denoted F1A and F2A.

(All these mixtures are listed in Table 4).

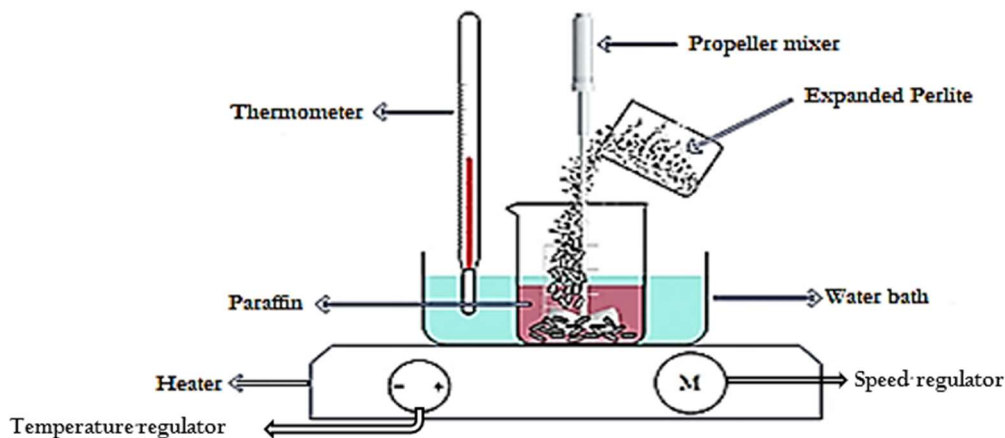


Figure 2. Direct impregnation of expanded perlite with paraffin.

Table 4. Summary of sample compositions for PCM composites.

Sample	Paraffin (g)	Expanded Perlite (g)	Cu (% Volume)	Epoxy Resin (g)
F1	60	40	0	0
F2	80	20	0	0
F1A	60	40	0.4	0
F2A	80	20	0.4	0
F1A Ep	60	40	0.4	150
F2A Ep	80	20	0.4	150

2.2.2. Step 2: Epoxy Coating of F1, F2, F1A and F2A

To prevent paraffin leakage, F1, F2, F1A and F2A have been coated with epoxy resin. Each of these will be mixed with one and a half parts epoxy resin by weight (1/1.5). The mixture starts by carefully mixing the two resin components (A and B) according to the supplier (1 part A and 1/2 part B by weight) with a spatula for 7 min, before adding the formulations (F1, F2, F1A and F2A) in small quantities while mixing manually with a spatula for 13 min, then the mixture is divided into several small parts and poured onto Teflon paper so that they don't stick together, after 48 h the mixtures obtained are coarsely ground and graded: F1 Ep, F2 Ep and F1A Ep and F2A Ep. (Note: These mixtures were prepared only with activated perlite and are also listed in Table 4).

2.2.3. Step 3: Mixing the Previously Prepared Compositions with HDPE on the Brabender Plastograph

The compositions thus prepared are mixed with HDPE on a Brabender plastograph at 180 °C with a speed of 40 rpm for 5 min, according to the compositions summarized in the Table 5:

(It should be noted that the mixes prepared with HDPE only concern those prepared with activated perlite, whose paraffin proportions are 80%). It is essential to understand that when using the plastograph for preparing blends, mixing constituents effectively requires working by volume. Specifically, the plastograph chamber, which has a capacity of 55 cm³, must be filled for any formulation. Consequently, the density of the constituents must be known or calculated, either manually or theoretically. In our case, we determined the required mass of HDPE to fill the chamber to be 44 g, indicating a density of the molten HDPE of 0.8 g/cm³. Based on this, we developed our mixes, ensuring that the chamber was always full. Thus, for each reduction in HDPE, it was replaced by an equivalent volume of F1, F2, F2A, or F2A Ep.

Table 5. The different mixes prepared with HDPE on the Plastograph.

HDPE (g)	Perlite (g)	F1 (g)	F2 (g)	F2A (g)	F2A Ep (g)
44	-	-	-		
42	2g	-	-		
42		4			
42			4		
34			6		
30			12		
36				6	
30				12	
36					6
30					12

Footnote: The required mass of HDPE to fill the chamber has been determined to be 44 g. This indicates that the density of molten is 0.8 g/cm³.

2.3. Technical Characterization

Several techniques were employed in this study to characterize the prepared composites and their constituent materials:

The paraffin leakage rate was evaluated using a weight loss method to analyze the phase stability of the samples under thermal conditions. Samples containing known percentages of paraffin were initially weighed using an analytical balance with a precision of four decimal places, ensuring high measurement accuracy. These samples were then subjected to various temperatures in an oven and exposed for different durations, allowing a comprehensive evaluation of the effect of these parameters on paraffin leakage. After cooling to room temperature, the samples were reweighed, and the mass difference was used to calculate the leakage rate for each tested condition. To verify the reliability of this method, the results were confirmed by Differential Gravimetric Analysis (DGA), performed using a TA Q600 instrument under a nitrogen atmosphere. This analysis covered a temperature range of 20 to 600 °C with a heating rate of 20 °C/min.

The thermal properties of the materials were studied using Differential Scanning Calorimetry (DSC) with a Perkin Elmer DSC 4000 instrument supplied by the authorized distributor in Tunis, Tunisia. The melting temperatures and enthalpies of fusion of pure paraffin were measured at heating rates of 5 °C/min and 10 °C/min, covering a temperature range from 20 °C to 90 °C. For HDPE-based blends, the analysis was extended to 180 °C with a heating rate of 10 °C/min. A nitrogen atmosphere was used during these tests to prevent oxidation.

The thermal stability of the composites was assessed using the same TA Q600 instrument, supplied by TA Instruments in Antwerp, Belgium, ensuring consistent conditions for studying mass loss and thermal degradation across the temperature range of 20 to 600 °C.

Thermo-physical properties, including the thermal conductivity, thermal diffusivity, and heat capacity of the composites, were measured using a Hot Disk TPS 500 thermal analyzer, supplied by Thermoconcept, Merignac, France. The instrument operated over a temperature range of 100 °C to 200 °C, with precision levels of 0.03 to 100 W·m⁻¹·K⁻¹ for thermal conductivity and 0.02 to 40 mm²/s for thermal diffusivity.

Finally, the morphology of the samples was observed using a scanning electron microscope (Joel Neoscope JSM-IT510) with a magnification range from 10× to 20,000×, supplied by JOEL in Croissy-sur-sein, France.

Each method was carefully selected to provide complementary and detailed insights into the physical, thermal, and structural properties of the composites studied. The analysis results are detailed and discussed in the following sections.

3. Results and Discussion

3.1. Paraffin Leakage Test Using the Weight Loss Method

When evaluating paraffin loss in composites, it is crucial to consider the moisture loss from perlite, which has a high moisture absorption capacity and can significantly impact the results. Consequently, the total measured weight loss reflects both the paraffin loss and the moisture released from the perlite.

To ensure accurate results, the calculation is conducted in two steps:

1. Determining the moisture loss from pure perlite as a function of temperature and time.
2. Subtracting the calculated moisture loss from the total weight loss measured for the composites.
 - a. Moisture loss in pure perlite:

$$\Delta m_{moisture}(T, t) (\%) = \frac{m_i - m_f}{m_i} \times 100 \quad (1)$$

where:

- m_i : initial mass of the perlite before heating.
- m_f : mass of the perlite after heating at temperature T for time t .

- b. Corrected paraffin loss for composites:

$$\Delta m_{paraffin,corrected}(T, t) (\%) = \Delta m_{composite}(T, t) - \Delta m_{moisture}(T, t) \quad (2)$$

where:

- $\Delta m_{composite}(T, t)$: total weight loss measured for the composite
- $\Delta m_{moisture}(T, t)$: moisture loss calculated for pure perlite.

Important Notes:

1. The values of $\Delta m_{paraffin,corrected}(T, t)$ are calculated by subtracting the moisture loss from the total weight loss of the composites.
2. No weight loss was recorded for the 60/40 paraffin/perlite ratio.
3. The units for both formulas are expressed as percentage (%), as they represent relative weight loss compared to the initial mass.

According to Table 6, moisture loss from perlite increases as a function of time and temperature, with a maximum loss of 2.94% at 60 °C. However, for the compounds (Table 7), paraffin leakage is almost insignificant, below 1.5% for coated compounds and below 2% for uncoated compounds. This leads us to conclude that the resin has correctly enveloped the composite, and that the small quantities recorded as leaking originate from the paraffin present on the perlite surface.

Table 6. Moisture loss in pure perlite ($\Delta m_{moisture}(T, t)$, in %).

	$T = 30\text{ °C}$	$T = 40\text{ °C}$	$T = 60\text{ °C}$
1 h	0.00 ± 0.00	0.00 ± 0.00	0.00 ± 0.00
2 h	0.37 ± 0.02	0.63 ± 0.04	2.02 ± 0.12
6 h	1.06 ± 0.06	1.36 ± 0.08	2.05 ± 0.12
24 h	2.35 ± 0.13	2.38 ± 0.14	2.94 ± 0.18

Table 7. Corrected paraffin loss in various compounds over time at different temperatures, in %.

Time	PCM/Perlite (80/20)								
	$T = 30\text{ °C}$			$T = 40\text{ °C}$			$T = 60\text{ °C}$		
	Δm_1	Δm_2	Δm_3	Δm_1	Δm_2	Δm_3	Δm_1	Δm_2	Δm_3
1 h	0.00	0.00	0.00	0.00 ± 0.00	0.15 ± 0.01	0.17 ± 0.01	0.56 ± 0.01	0.37 ± 0.01	0.55 ± 0.01
2 h	0.00	0.00	0.00	0.15 ± 0.04	0.21 ± 0.04	0.23 ± 0.04	1.76 ± 0.12	1.36 ± 0.12	1.41 ± 0.12
6 h	0.00	0.00	0.00	0.28 ± 0.08	0.35 ± 0.08	0.41 ± 0.08	1.85 ± 0.12	1.09 ± 0.12	1.04 ± 0.12
24 h	0.00	0.00	0.00	0.78 ± 0.14	0.42 ± 0.14	0.51 ± 0.014	1.98 ± 0.18	1.13 ± 0.18	1.44 ± 0.18

Where: Δm_1 : Corrected paraffin loss for the PCM/Exp (paraffin/Expanded Perlite) composite; Δm_2 : Corrected paraffin loss for the PCM/Exp/Epoxy composite; Δm_3 : Corrected paraffin loss for the PCM/Exp/Epoxy/Cu composite.

3.2. Morphological Analysis by Scanning Electron Microscope (SEM)

In order to examine the morphology of pure, untreated and treated perlite as well as the different compositions prepared, we carried out observations by scanning electron microscopy.

The figures below show the different SEM photographs obtained for UnExP and TExP and their composites.

Figure 3a, shows that UnExP appears in a variety of angular shapes, with clearly visible pores and very thin walls. On the other hand, Figure 3b shows that the microstructure of TExP is made up of smaller sheets, probably due to chemical treatment with HCl.

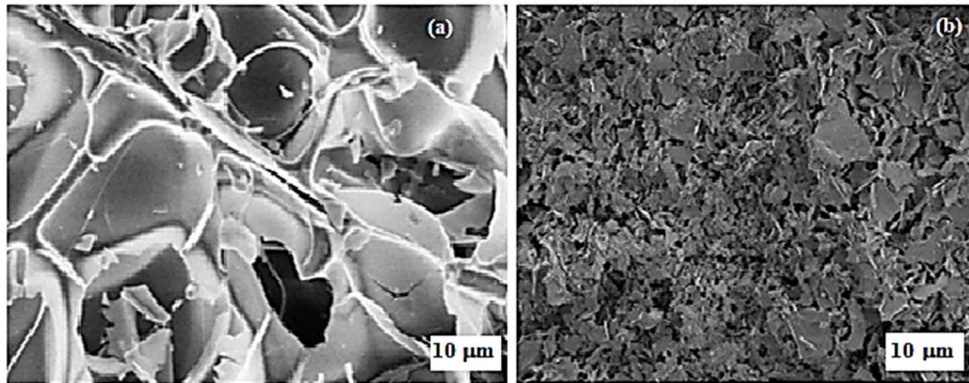


Figure 3. SEM photographs of UnExP (a), TExP (b).

Figure 4a shows that the perlite pores are empty, while in Figure 4b, the UnExP microstructure is well impregnated with PCM and the absence of cracks indicates that the latter has adhered well to the UnExP. In Figure 4c, the epoxy coating is clearly visible.

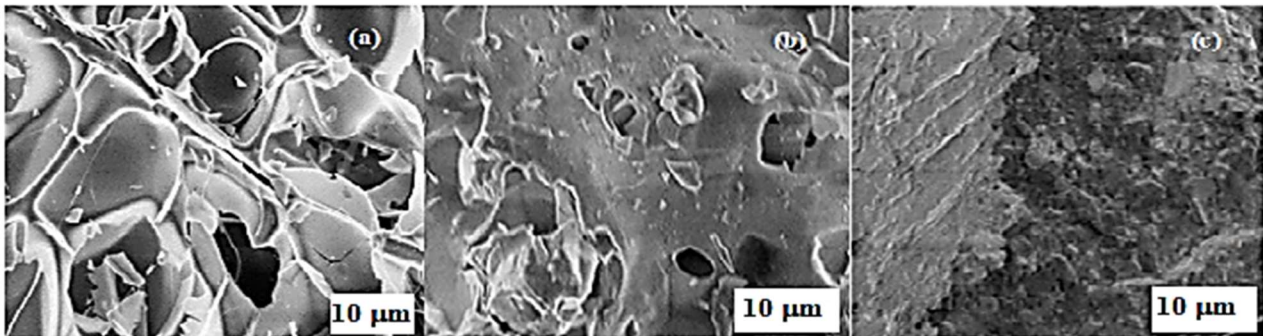


Figure 4. SEM photographs of UnExP (a), PCM/UnExP (b) and PCM/UnExP/Ep (c).

Figure 5b clearly shows that the Paraffin has adhered well to the perlite and appears compact, while the brightness of the PCM/TExP/Ep composites in Figure 5c clearly indicates that the addition of the epoxy covers all the materials (PCM/TExP) to form a compact mass.

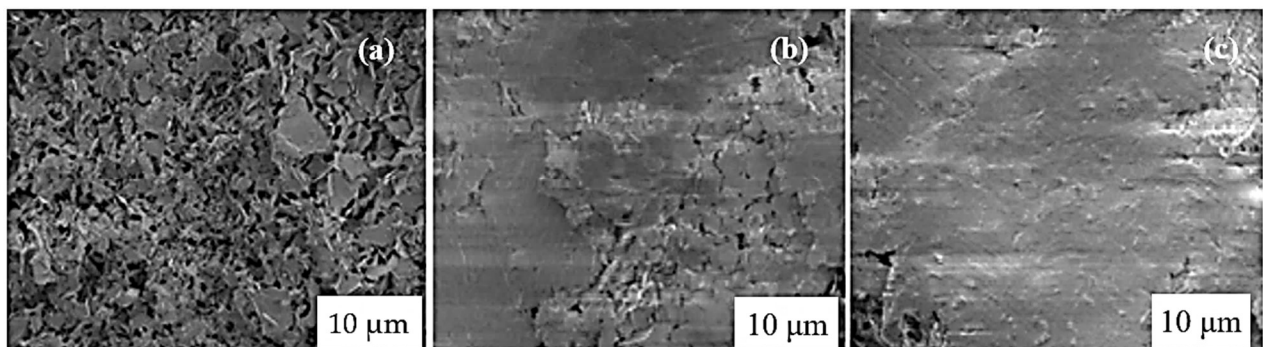


Figure 5. SEM photographs of TExP (a), PCM/ TExP (b), (PCM/TExP/Ep) (c).

Figure 6 shows the two photographs illustrating the effect of the amount of paraffin added. In the 60/40 ratio, the paraffin is absorbed by the perlite, but the low paraffin-to-perlite ratio limits the uniform absorption capacity. When the

amount of paraffin is insufficient to fill all the pores of the perlite, some of it becomes concentrated locally, forming agglomerates. These agglomerates are likely the result of localized saturation, where the perlite reaches its maximum absorption capacity and can no longer take in any more paraffin, leading to the formation of visible clusters. In contrast, in the 80/20 ratio, the amount of paraffin is higher, allowing the perlite to fill more of its pores in a more uniform manner. When the amount of paraffin exceeds the perlite's absorption capacity, an excess of paraffin may form in the interstices, thus contributing to a more compact structure. This observation shows that the amount of paraffin plays a crucial role in determining the final morphology of the composite: a larger amount of paraffin promotes a denser and more homogeneous structure, demonstrating the increased capacity of the perlite to absorb paraffin when it is present in sufficient quantity.

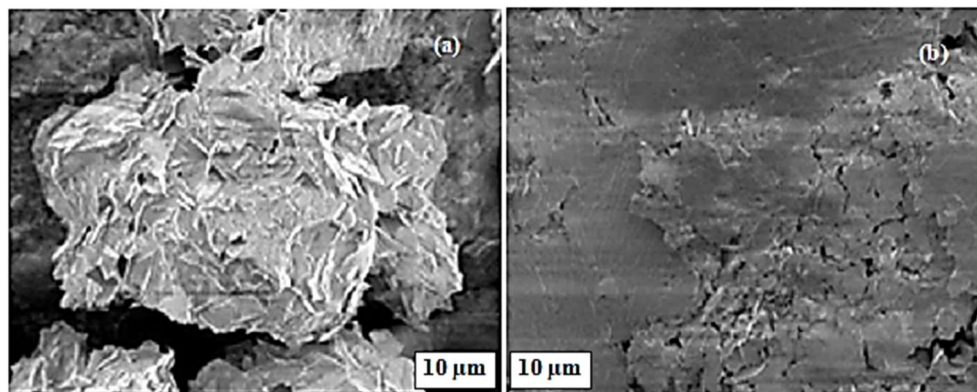


Figure 6. Micrographs showing morphological differences in the PCM/TEXP mixture, containing the proportions of 60/40 (a) and 80/20 (b).

3.3. Thermogravimetric Analysis (TGA)

The TGA thermogram of pure perlite Figure 7, shows that perlite is very stable in the studied range (25–600 °C) and that the 3% loss by mass corresponds to the existing moisture in its pores.

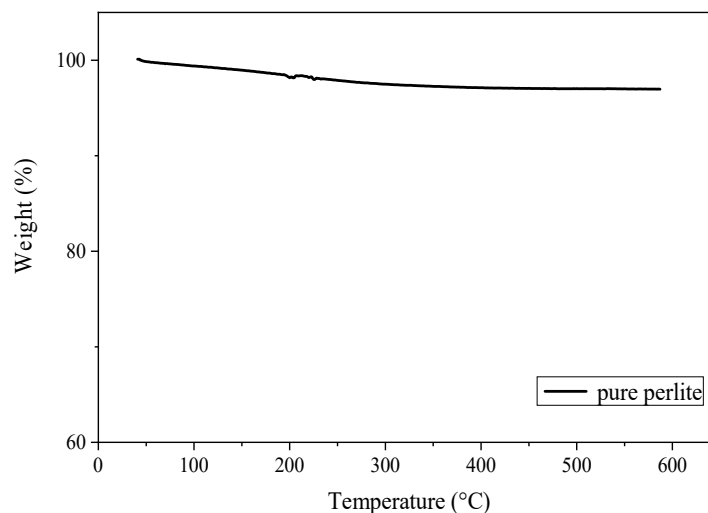


Figure 7. TGA thermograms of pure expanded perlite.

From Figure 8, it can be seen that epoxy decomposition takes place in two steps, the 1st step is attributed to its flash point starting from 118 °C and ending at 324 °C, the 2nd step starting from 324 °C and ending after total degradation at around 498 °C, with a maximum mass loss of 96%.

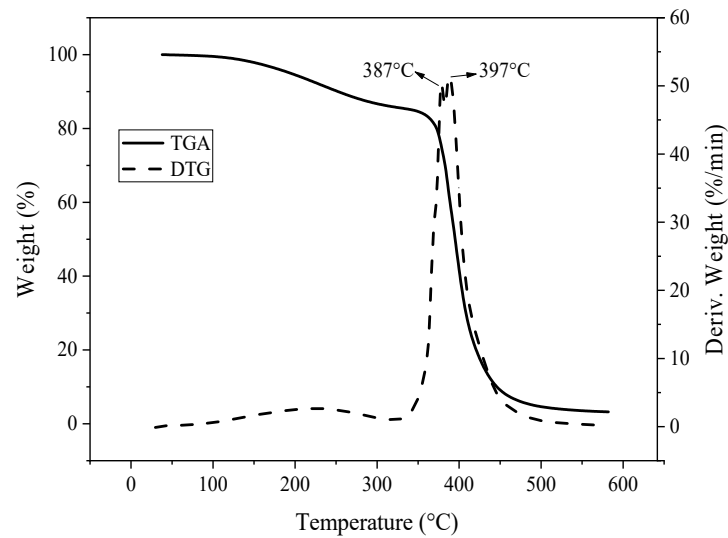


Figure 8. Epoxy TGA-DTGA thermogram.

Figures 9 and 10 highlight the significant impact of HCl treatment on the properties of composites based on perlite and paraffin. By comparing untreated perlite (UnExP) and HCl-treated perlite (TExP) with a Perlite/Paraffin ratio of 60/40, it is evident that the HCl treatment significantly enhances the paraffin adsorption capacity and thermal stability of the composite. The untreated composite shows a total weight loss of 55%, while the treated composite reaches 60%. This increase indicates that the chemical treatment removes impurities from the perlite surface, increasing the active sites available for paraffin adsorption. Furthermore, the thermal degradation temperature of the treated composite is higher (299.44 °C) compared to the untreated composite (292 °C). This improvement is attributed to the increased purity of the perlite and the higher amount of adsorbed paraffin, which together enhance thermal stability. These results underscore the importance of HCl treatment in improving composite performance, particularly regarding paraffin storage capacity and thermal resistance, which are crucial for advanced thermal applications.

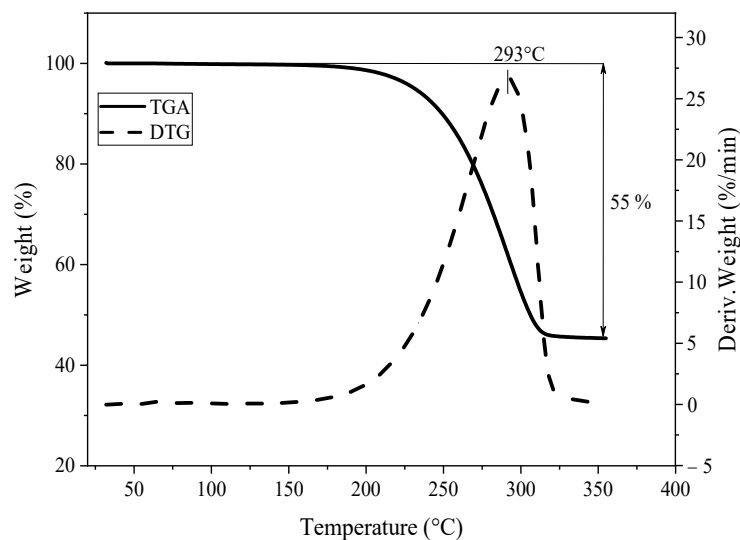


Figure 9. TGA-DTGA thermograms of PCM/UnExP mixture (60/40).

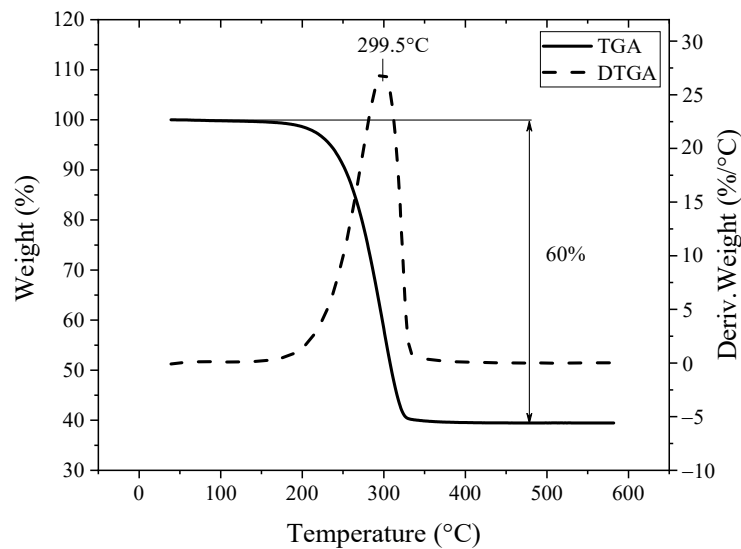


Figure 10. TGA-DTG thermograms of PCM/TEXP mixture (60/40).

In comparison, while Ramakrishnan and Mekaddem [19,20] also studied composites based on perlite and paraffin for thermal energy storage, their works did not consider the impact of chemical treatment on perlite. Ramakrishnan et al. achieved a paraffin content of 50%, and Mekaddem et al. reached 60%. Our study, however, stands out by achieving a paraffin content of 80%, highlighting the role of HCl treatment in enhancing perlite's adsorption capacity and improving composite performance.

Moreover, the incorporation of high-density polyethylene into our composites adds an additional layer of innovation by improving mechanical properties and durability. Unlike earlier studies, which focused primarily on impermeability and thermal conductivity, our research broadens the application scope of these materials, particularly in the construction sector, with potential uses in windows, doors, plasters, and cements.

Figure 11, showing the PCM/TEXP composite (80/20), shows that decomposition takes place in two steps, the first with a maximum degradation temperature of 278.5 °C and the second with a maximum degradation temperature of 328.5 °C. This can probably be attributed to the degradation of the surface paraffin, followed by the degradation of the paraffin in the deeper pores. With a total mass loss of 82%, corresponding to the incorporated paraffin and the moisture content of the composite, which is 2%.

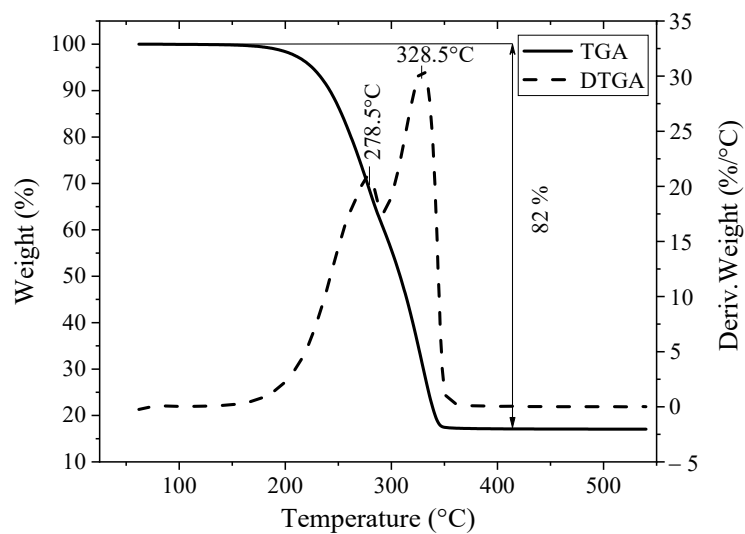


Figure 11. TGA-DTGA thermograms of PCM/TEXP mixture (80/20).

Figure 12, representing the PCM/TEXP/Ep composite ratio (80/20), shows that decomposition takes place in two steps, the first has a maximum degradation temperature equal to 300.8 °C, attributed to paraffin degradation, while the second one has a maximum decomposition temperature of 386.6 °C attributed to Epoxy resin decomposition, with a total mass loss of 76%. The difference in behavior observed between the PCM/TEXP composite and the PCM/TEXP/Ep

composite, illustrated in Figures 11 and 12 respectively, can be attributed to the presence of the epoxy resin. Indeed, the epoxy acts as a thermal barrier, thus delaying the degradation of the paraffin and introducing a second phase of decomposition specific to the epoxy. This shows that the epoxy influences not only the thermal stability of the PCM but also plays a central role in the overall thermal behavior of the composite.

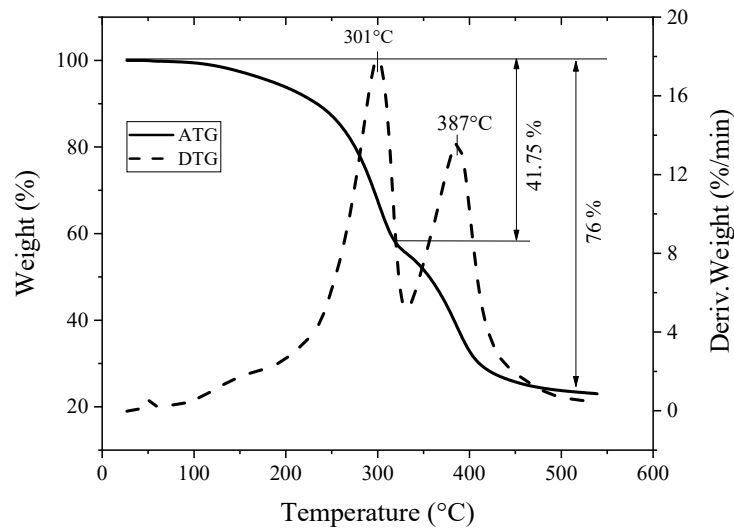


Figure 12. TGA-DTGA thermograms of (PCM/TEXP/Epoxy) mixture, with (PCM/TEXP) 80/20.

3.4. Differential Scanning Calorimetry (DSC) Analysis

The DSC thermogram clearly shows two melting peaks during heating and two crystallization peaks during cooling for RT55 paraffin (Figure 13). The first peak, of low amplitude, and the second, of higher amplitude, indicate that the paraffin is composed of a mixture of hydrocarbons with different molecular weights. As reported by [20], the first peak may be attributed to a solid-solid transition. Furthermore, the analysis reveals that slower heating rates lead to higher crystallization temperatures and lower melting temperatures. This behavior can be explained by the fact that lower heating rates allow more time for the formation of stable crystalline structures, thus increasing the crystallization temperature. Conversely, during melting, slower heating reduces the energy required for the solid-liquid transition, thus lowering the melting temperature. For HDPE blends, it should be remembered that only the 80/20 (PCM/ExP) ratio was chosen in this study. From the thermograms (Figure 14) and Table 8, it was noted that the melting temperatures of HDPE decrease compared to pure HDPE. This decrease varies from 4.72 °C for HDPE/(PCM/ExP/Ep) blends with a 34 g/6 g ratio to 9.58 °C for HDPE/(PCM/ExP) blends with a 30 g/12 g ratio. This phenomenon could be attributed to the interactions between HDPE and the additives present in the blends, such as epoxy and copper, which influence molecular mobility and thus modify the thermal transitions. An increase in the melting enthalpy of HDPE was also observed. This could be explained by the protective effect of epoxy and copper, which strengthen the HDPE structure and increase the energy required for its melting. This increase could also indicate higher crystallinity of HDPE in the blends, a point that would merit further investigation. Regarding paraffin in the blends, the results show a decrease in its melting temperatures and a slight increase in its crystallization temperatures. However, the transition peaks associated with paraffin become minimal, particularly in composites containing epoxy, where they become almost undetectable. This phenomenon could be attributed to the dominant presence of HDPE or to a non-homogeneous distribution of paraffin in the matrix. This observation significantly complicates the calculation of paraffin transitions, justifying the exclusion of these results from this analysis. The comparison between the different ratios (34 g/6 g and 30 g/12 g) highlights the impact of proportions on thermal transitions. The addition of epoxy and copper seems to play a key role in influencing crystallization kinetics, as evidenced by slight increases in crystallization temperatures in all blends. This phenomenon could be due to a nucleation effect induced by these additives, favoring the formation of crystalline structures. Finally, the difficulty in detecting the thermal transitions of PCM in the composites is likely due to the amount of paraffin present in the composite or the overlap of PCM thermal transitions with those of the other components.

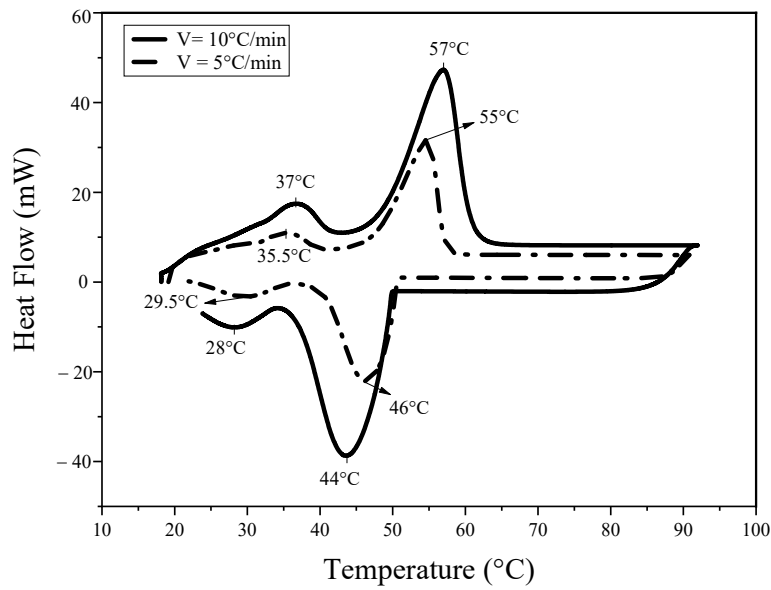


Figure 13. DSC thermogram of Paraffin RT55 at two heating rates.

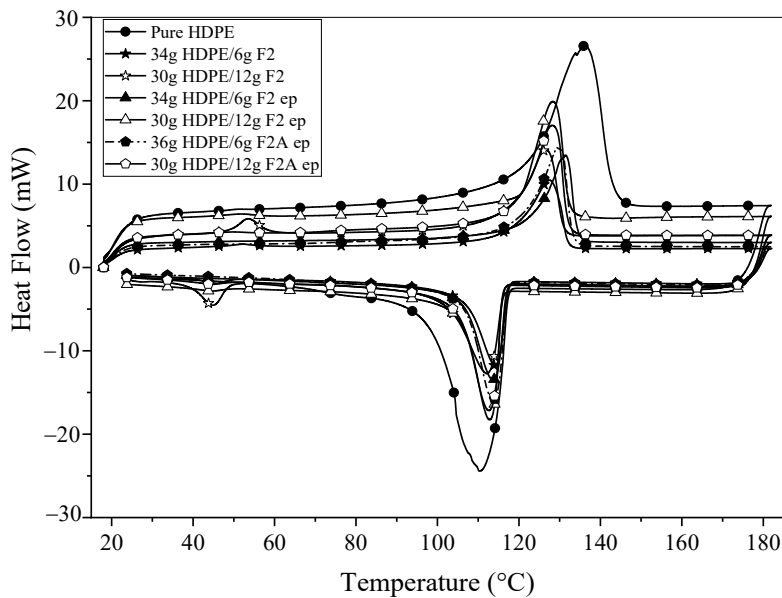


Figure 14. DSC thermograms of HDPE mixtures.

Table 8. DSC results taking into account the proportions of HDPE and paraffin (PCM) in the mixtures.

Mixtures	T _m PCM (°C)	T _c PCM (°C)	ΔH _m PCM (J/g)	ΔH _c PCM (J/g)	T _m HDPE (°C)	T _c HDPE (°C)	ΔH _m HDPE (J/g)	ΔH _c HDPE (J/g)
Pure PCM (v = 5 °C/min)	54.84	46.36	121.71	138.23				
Pure PCM (v = 10 °C/min)	56.98	43.67	119.5	133.27				
Pure HDPE					136.22	110.34	151.66	158.53
HDPE/(PCM/ExP) 34 g/6 g	52.25	45.70	4.24	8.41	127.46	114.15	141.25	115.85
HDPE/(PCM/ExP) 30 g/12 g	53.64	44.88	53.94	92.11	126.64	112.13	134.51	138.75
HDPE/(PCM/ExP/Ep) 34 g/6 g	/	/	/	/	131.50	113.7	151.20	145.27
HDPE/(PCM/ExP/Ep) 30 g/12 g	52	44.7	0.82	0.51	128.43	112.84	135.12	155.58
HDPE/(PCM/ExP/Ep/Cu) 36 g/6 g	/	/	/	/	129.80	113.70	151.19	128.25
HDPE/(PCM/ExP/Ep/Cu) 30 g/12 g	50	44.73	0.30	0.66	128.20	112.70	174.90	159.34

Note: T_m PCM: Melting temperature of the PCM. T_c PCM: Crystallization temperature of the PCM. ΔH_m PCM: Heat of fusion of the PCM. ΔH_c PCM: Heat of crystallization of the PCM. T_m HDPE: Melting temperature of the HDPE. T_c HDPE: Crystallization temperature of the HDPE. ΔH_m HDPE: Heat of fusion of the HDPE. ΔH_c HDPE: Heat of crystallization of the HDPE.

3.5. Thermophysical Properties

Based on the results summarized in Table 9, it was observed that thermal conductivity remained relatively stable across the various blends, except for the 34 g/6 g composition, which showed an increase of approximately 9% compared to pure HDPE. These findings indicate that the amount of (PCM/ExP/ep) added to HDPE is very small, explaining the slight variation in thermal conductivity observed. However, a slight decrease in thermal diffusivity was noted, particularly in the HDPE/(PCM/ExP) (30 g/12 g) and HDPE/(PCM/ExP/ep) (30 g/12 g) blends. This reduction in diffusivity can be attributed to the interference of perlite with the molecular structure of HDPE, hindering thermal conduction through the composite. Furthermore, the interface between HDPE and perlite creates a barrier to heat transfer, further reducing thermal diffusivity. The presence of voids, defects, or inhomogeneities within the composite may also contribute to thermal resistance, impeding efficient heat transfer and resulting in lower thermal diffusivity compared to pure HDPE.

Table 9. Thermo-physical properties of prepared mixtures.

Mixtures	Thermal Conductivity (W/m·K)	Thermal Diffusivity (mm ² /s)	Specific Heat (MJ/m ³ ·K)
Pure HDPE	0.45	0.30	1.51
HDPE/(PCM/ExP) 36 g/6 g	0.45	0.27	1.76
HDPE/(PCM/ ExP) 30 g/12 g	0.46	0.25	1.80
HDPE/(PCM/ ExP/ep) 34 g/6 g	0.49	0.31	1.40
HDPE/(PCM/ ExP/ep) 30 g/12 g	0.434	0.25	1.72
HDPE/(PCM/ ExP/ep/Cu) 36 g/6 g	0.454	0.28	1.57
HDPE/(PCM/ ExP/ep/Cu) 30 g/12 g	0.438	0.28	1.48

4. Conclusions

In summary, this study presents the development and analysis of an innovative and shape-stable phase-change material (PCM), combining expanded perlite, paraffin, copper, epoxy resin, and high-density polyethylene (HDPE), designed for thermal energy storage and release. Rigorous leakage and weight loss tests demonstrated that perlite effectively absorbed paraffin, while the epoxy resin provided a protective coating, preventing any paraffin leakage. Thermogravimetric analysis (TGA) confirmed that hydrochloric acid (HCl) treatment significantly improved the absorption capacity of perlite, achieving up to 80% by weight, surpassing the results reported in the studies of Ramakrishnan and Mekaddem, who were limited to 50% and 60%, respectively. The HCl treatment thus demonstrated its effectiveness in increasing perlite's absorption capacity.

The integration of HDPE into the composite acted as an additional protective layer, enhancing the material's mechanical properties and expanding its range of applications, particularly in the construction sector. This composite could thus be incorporated into PVC windows and doors, as well as plaster and cement.

Scanning electron microscopy (SEM) observations showed that the 80/20 paraffin-to-perlite ratio produced a more compact structure compared to the 60/40 ratio, which exhibited agglomerates. The glossy appearance observed in the SEM images confirmed the insulating role of the epoxy resin. Differential scanning calorimetry (DSC) results revealed slight variations in the melting temperature of paraffin when mixed with HDPE, while its crystallization temperature remained almost constant. Thermal conductivity remained relatively stable across the different compositions, with a 9% increase observed in the 34 g/6 g composition. This limited variation in conductivity suggests that increasing the amount of (PCM/ExP/ep) in the HDPE/(PCM/ExP/ep/Cu) composite would be necessary to optimize its thermal performance. Finally, a slight decrease in thermal diffusivity was noted, likely due to the interaction between perlite and the molecular structure of HDPE.

Overall, this PCM-based composite shows great potential for thermal energy storage, making it an excellent candidate for high-efficiency building materials, particularly for applications similar to advanced materials such as ALUCOBOND.

Acknowledgments

We would like to express our sincere gratitude to Salwa Bouadila, at the Center for Research and Energy Technologies, Hammam Lif—Tunisia, for her valuable assistance in conducting the DSC tests and the thermal property tests (Hot Disk).

Author Contributions

L.G. carried out 90% of the work, including developing the research idea, designing the work plan, conducting the theoretical and experimental work, and interpreting the results. F.R. contributed specifically to the interpretation of the thermal properties results (Hot Disk).

Ethics Statement

As our study does not involve humans or animals, ethical approval is not required.

Informed Consent Statement

Not applicable.

Funding

This research received no external funding.

Declaration of Competing Interest

The authors declare that they have no known competing financial interests or personal relationships that could have appeared to influence the work reported in this paper.

References

1. Sarbu I, Sebarchievici C. Comprehensive Review of Thermal Energy Storage. *Sustainability* **2018**, *10*, 191.
2. Shchukina EM, Graham M, Zheng Z, Shchukin DG. Nanoencapsulation of phase change materials for advanced thermal energy storage systems. *Che. Soc. Rev. J.* **2018**, *47*, 4156–4175.
3. Drissi S, Ling T-C, Mo KH, Eddahhak A. A review of microencapsulated and composite phase change materials: Alteration of strength and thermal properties of cement-based materials. *Renew. Sustain. Energy Rev.* **2019**, *110*, 467–484.
4. de Gracia A, Cabeza LF. Phase change materials and thermal energy storage for buildings. *Energy Build.* **2015**, *103*, 414–419.
5. Zhu N, Li S, Hu P, Wei S, Deng R, Lei F. A Review on applications of shape-stabilized phase change materials embedded in building enclosure in recent ten years. *Sustain. Cities Soc.* **2018**, *43*, 251–264.
6. Fantini P. Phase Change Memory Applications: The History, the Present and the Future. *J. Phys. D Appl. Phys.* **2020**, *53*, 283002.
7. Kheradmand M, Azenha M, De Aguiar JLB, Castro-Gomes J. Experimental and Numerical Studies of Hybrid PCM Embedded in Plastering Mortar for Enhanced Thermal Behaviour of Buildings. *Energy* **2016**, *94*, 250–261.
8. Guarino F, Athienitis A, Cellura M, Bastien D. PCM Thermal Storage Design in Buildings: Experimental Studies and Applications to Solaria in Cold Climates. *Appl. Energy* **2017**, *185*, 95–106.
9. Nazir H, Batool M, Bolivar Osorio FJ, Isaza-Ruiz M, Xu X, Vignarooban K, et al. Recent developments in phase change materials for energy storage applications. *Int. J. Heat Mass Transf.* **2019**, *129*, 491–523.
10. Li Y, Nord N, Xiao Q, Tereshchenko T. Building Heating Applications with Phase Change Material: A Comprehensive Review. *J. Energy Storage* **2020**, *31*, 101634.
11. Bouhal T, El Rhafiki T, Kousksou T, Jamil A, Zeraouli Y. PCM Addition inside Solar Water Heaters: Numerical Comparative Approach. *J. Energy Storage* **2018**, *19*, 232–246.
12. Bak A, Pławecka K, Łach M. Comparison of Thermal Conductivity of Foamed Geopolymers Containing Phase Change Materials. *J. Phys. Conf. Ser.* **2023**, *2423*, 012003.
13. Somani P, Gaur A. Evaluation and Reduction of Temperature Stresses in Concrete Pavement by Using Phase Changing Material. *Mater. Today Proc.* **2020**, *32*, 856–864.
14. Partl MN. Quest for Improving Service Life of Asphalt Roads. *RILEM Tech. Lett.* **2020**, *4*, 154–162.
15. Mehling H, Brütting M, Haussmann T. PCM Products and Their Fields of Application—An Overview of the State in 2020/2021. *J. Energy Storage* **2022**, *51*, 104354.
16. Li F, Zhou S, Chen S, Yang J, Zhu X, Du Y, et al. Low-Temperature Organic Phase Change Material Microcapsules for Asphalt Pavement: Preparation, Characterization and Application. *J. Microencapsul.* **2018**, *35*, 635–642.
17. Korniejenko K, Nykiel M, Aruova L, Choinska M, Jexembayeva A, Konkanov M. An Overview of Phase Change Materials and Their Applications in Pavement. *Energies* **2024**, *17*, 1–18.
18. Tach M, Pławecka K, Bąk A, Adamczyk M, Bazan P, Kozub B, et al. Review of Solutions for the Use of Phase Change Materials in Geopolymers. *Materials* **2021**, *14*, 6044.
19. Ramakrishnan S, Sanjayan J, Wang X, Alam M, Wilson J. A novel paraffin/expanded perlite composite phase change material for prevention of PCM leakage in cementitious composites. *Appl. Energy* **2015**, *157*, 85–94.

20. Mekaddem N, Ben Ali S, Fois M, Hannachi A. Paraffin/Expanded Perlite/Plaster as Thermal Energy Storage Composite. *Energy Proced.* **2019**, *157*, 1118–1129.
21. Bayés-García L, Ventolà L, Cordobilla R, Benages R, Calvet T, Cuevas-Diarte MA. Phase Change Materials (PCM) microcapsules with different shell compositions: Preparation, characterization and thermal stability. *Sol. Energy Mater. Sol. Cells* **2010**, *94*, 1235–1240.
22. Rubitherm Technologies GmbH. Available online: <http://www.rubitherm.com/S> (accessed on 7 January 2023).
23. SARL TAOUAB. Perlite Construct, Poudre, Kouba, Alger. Available online: https://www.taouab.com/powder_details.html (accessed on 13 February 2021).
24. SABIC®. *SABIC® HDPE*. Available online: <https://www.sabic.com/en/products/polymers/polyethylene-pe/sabic-hdpe> (accessed on 17 January 2023).